SCIENTIFIC REPORTS

OPEN

SUBJECT AREAS:
CHEMISTRY
PHYSICAL CHEMISTRY

Received
30 May 2014

Accepted
2 September 2014

Published
23 September 2014

Correspondence and requests for materials should be addressed to B.Z. (zhangbin@iccas.ac.cn)

Candidate Quantum Spin Liquid due to Dimensional Reduction of a Two-Dimensional Honeycomb Lattice

Bin Zhang[1], Yan Zhang[2], Zheming Wang[3], Dongwei Wang[4], Peter J. Baker[5], Francis L. Pratt[5] & Daoben Zhu[1]

[1]Organic Solid Laboratory, BNLMS, CMS & Institute of Chemistry, Chinese Academy of Sciences, Beijing, 100190, P. R. China, [2]Institute of Condensed Matter Physics, College of Physics, Peking University, Beijing, 100871, P. R. China, [3]BNLMS, College of Chemical and Molecular Engineering, Peking University, 100871, P. R. China, [4]National Center for Nanoscience and Nanotechnology, Beijing, 100190, P. R. China, [5]ISIS Facility, STFC Rutherford Appleton Laboratory, Harwell Science and Innovation Campus, Didcot, OX11 0QX, United Kingdom.

As with quantum spin liquids based on two-dimensional triangular and kagome lattices, the two-dimensional honeycomb lattice with either a strong spin-orbital coupling or a frustrating second-nearest-neighbor coupling is expected to be a source of candidate quantum spin liquids. An ammonium salt $[(C_3H_7)_3NH]_2[Cu_2(C_2O_4)_3](H_2O)_{2.2}$ containing hexagonal layers of Cu^{2+} was obtained from solution. No structural transition or long-range magnetic ordering was observed from 290 K to 2 K from single crystal X-ray diffraction, specific heat and susceptibility measurements. The anionic layers are separated by sheets of ammonium and H_2O with distance of 3.5 Å and no significant interaction between anionic layers. The two-dimensional honeycomb lattice is constructed from Jahn-Teller distorted Cu^{2+} and oxalate anions, showing a strong antiferromagnetic interaction between $S = 1/2$ metal atoms with $\theta = -120$ (1) K. Orbital analysis of the Cu^{2+} interactions through the oxalate-bridges suggests a stripe mode pattern of coupling with weak ferromagnetic interaction along the *b* axis, and strong antiferromagnetic interaction along the *a* axis. Analysis of the magnetic susceptibility shows that it is dominated by a quasi-one-dimensional contribution with spin chains that are at least as well isolated as those of well-known quasi-one-dimensional spin liquids.

Magnetic systems exhibit, most commonly, classical long-range order at low temperature. To avoid magnetic ordering the interactions between magnetic atoms can be frustrated by the topology of the underlying lattice and/or compete with one another, the dimensionality of the lattice can be reduced by weakening the interactions between planes or chains, or the spin of magnetic units can be reduced to $S = 1/2$ to promote quantum fluctuation[1–5]. Examples of geometric frustration include antiferromagnetic materials based on a triangular lattice or a Kagome lattice on which triangles share their corners rather than edges. For a perfect system, this frustration would result in the ground state being inherently highly degenerate, even a spin liquid state[3–5]. For real systems, the degree of frustration is described by the parameter $f = \theta_{CW}/T_N$, the Curie-Weiss temperature θ_{CW} showing how strong the magnetic interactions are and the Néel temperature T_N defining the onset of magnetic order. An unfrustrated system has $f = 1$, a spin frustrated system has $f \geq 10$ and in an ideal spin frustrated system f tends to infinity[2,3].

Quantum spin liquids have attracted particular attention since Anderson proposed their possible connection to the superconductivity of cuprates[6,7]. But most compounds with triangular-lattices or Kagome lattices showed long-range magnetic order due to structural distortion or crystal defects[8–15]. So far, quantum spin liquid states were observed in four triangular lattice compounds, namely κ-$(BEDT\text{-}TTF)_2Cu_2(CN)_3$ (BEDT-TTF = bis(theylenedithio)tetrathiafulvalene), $(C_2H_5)(CH_3)_3Sb[Pd(dmit)_2]_2$ (dmit = 1,3-dithiole-2-thione-4,5-dithiolate), $H_3(Cat\text{-}EDT\text{-}TTF)_2$ and $LiZn_2Mo_3O_8$[16–19]. In kagome lattices, a stronger spin frustration is expected than for triangular lattices and quantum spin liquid states were observed in the two compounds $ZnCu_3(OH)_6Cl_2$ and $[NH_4]_2[C_7H_{14}N][V_7O_6F_{18}]$[20–23]. In one dimensional system including $KCuF_3$ and copper pyrazine dinitrate the spinon continuum associated with the spin liquid state has been observed directly and it has also been confirmed for the two-dimensional kagome system $ZnCu_3(OH)_6Cl_2$[22,24,25].

Quantum spin liquids with two-dimensional lattices should not only be limited to triangular lattices and Kagome lattices[2,26]. The $S = 1/2$ honeycomb lattice (Figure 1) with strong spin –orbital coupling described by

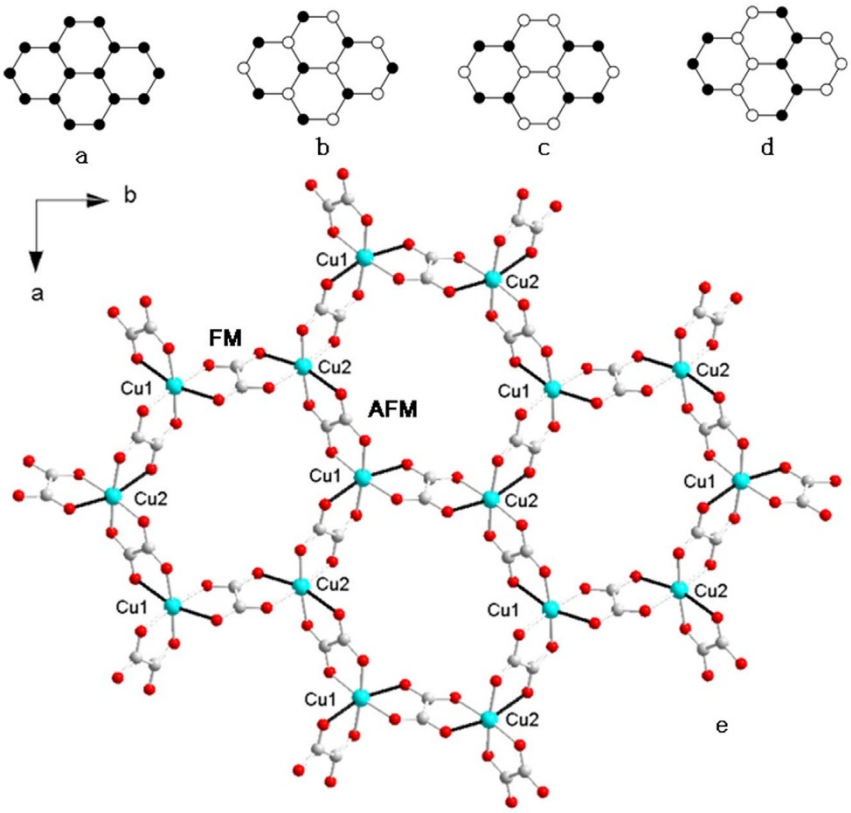

Figure 1 | A schematic of four magnetic configuration of honeycomb lattice: (a) the ferromagnetic state, (b) the Néel antiferromagnetic state, (c) the stripy antiferromagnetic state, (d) the zigzag antiferromagnetic state, and (e) arrangement of anionic layer on the *ab* plane at 290 K. Color code: Cu, blue; C, grey; O, red. White solid lines: Cu–O, C–C, C–O bond.

the exactly-solvable Kitaev honeycomb model has been proposed as a candidate quantum spin liquid and may exhibit Majorana Fermions that could enable future schemes for quantum computation[27–31]. This is an idealization of real systems where Heisenberg-like and next-nearest-neighbor J_2 coupling lead to an even richer assortment of phases, including other spin-liquids. However, the best-known model honeycomb compound Na_2IrO_3 shows long-range magnetic ordering at 13.3 K and other higher spin systems such as $Bi_3Mn_4O_{12}(NO_3)$, $Na_2Co_2TeO_6$, $Na_3Co_2SbO_6$, RNi_3Al_9, $Cu_3Ni_2SbO_6$, $Cu_2Co_2SbO_6$, and $Ba_3Co_2O_6(CO_3)_{0.2}$ – all order magnetically[32–37]. The quest for $S = 1/2$ honeycomb systems that exhibit strong magnetic frustration therefore continues to excite the physics community, and at the same time challenge the chemistry community.

In 2011, spin fluctuation was observed in a charge-transfer salt $(BEDT\text{-}TTF)_3[Cu_2(C_2O_4)_3](CH_3OH)_2$ with $S = 1/2$ Cu^{2+} forming a distorted honeycomb lattice, the Weiss constant was −29.8(7) K and there was no long-range magnetic ordering observed above 2 K[38]. Two sets of spins exist in this compound: one coming from the donor molecules is similar to the $S = 1/2$ triangular lattice in κ-$(BEDT\text{-}TTF)_2Cu_2(CN)_3$, the other coming from the anionic layer forming the $S = 1/2$ honeycomb lattice[16]. In order to focus on the properties of the $S = 1/2$ honeycomb lattice, an ammonium salt $[(C_3H_7)_3NH]_2[Cu_2(C_2O_4)_3](H_2O)_{2.2}$ (**1**) was synthesized and magnetic ordering was found to be strongly suppressed, setting a lower bound of 60 for the frustration parameter *f*.

Results

Temperature-dependent single crystal X-ray experiment. **1** crystallizes in a monoclinic system with cell parameters: a = 9.3696(1) Å, b = 16.0340(2) Å, c = 22.7991(4) Å, β = 92.9561(5) °, V = 3420.60(8) Å^3, $Z = 4$, at 290 K. Figure 2a shows the temperature dependent cell parameters from room-temperature to 100 K. When temperature decreased, the b and c axis contracted, the a axis and the β angle show a negative thermal expansion[39]. The negative thermal expansion coefficient as $\alpha_a \cong 1.9 \times 10^{-5}$ K^{-1} above 140 K, 1.5×10^{-5} K^{-1} between 140 K and 100 K, and $\alpha_\beta \cong 2.7 \times 10^{-5}$ K^{-1} above 140 K. Below 140 K, the β value decreased while temperature decreased. The b axis, the c axis and the volume decreased when temperature decreased, and the space group remained $P2_1/n$ in the X-ray diffraction experimental temperature range.

Crystal structure. At 290 K, there are two $(C_3H_7)_3NH^+$ in an asymmetric unit in **1**. One of the propyl groups connects to N1, points in the direction perpendicular to the *ab* plane and intercalates into a cavity of the anionic honeycomb. The non-hydrogen-atoms on the ammonium of N2 are almost parallel to the *ab* plane, the hydrogen bond between N–H and O of oxalate anion was found to be N2–H2···O10 2.806 Å/166.96°. H_2O molecules exist in five positions with populations of 0.50, 0.50, 0.50, 0.50 and 0.20, so there are 2.2 H_2O in an asymmetric unit. There are hydrogen bonds between cation and H_2O and between solvent and anionic layer. Two sheets of ammonium exist between the two anion layers and there is no weak interaction between ammoniums. This explains the nature of the crystal effectively, because it is always a thin plate crystal and cleaves easily (Figure S1).

In **1**, Cu is coordinated by three bisbidentated oxalate anions, Cu1 and Cu2 are neighboring to each other, so a (6,3) honeycomb network is formed on the *ab* plane. The Cu-O distances are 1.969(2) ~ 2.310(2) Å for Cu1 and 1.966(2) ~ 2.340(2) for Cu2, and the Cu–O distances on the equatorial plane are shorter than those in the axial direction as a result of the Jahn-Teller distortion. The elongated bonds on the Jahn-Teller distorted octahedron around the Cu^{2+} are highlighted with black solid lines (Figure 1e). The *cis*-O–Cu–O

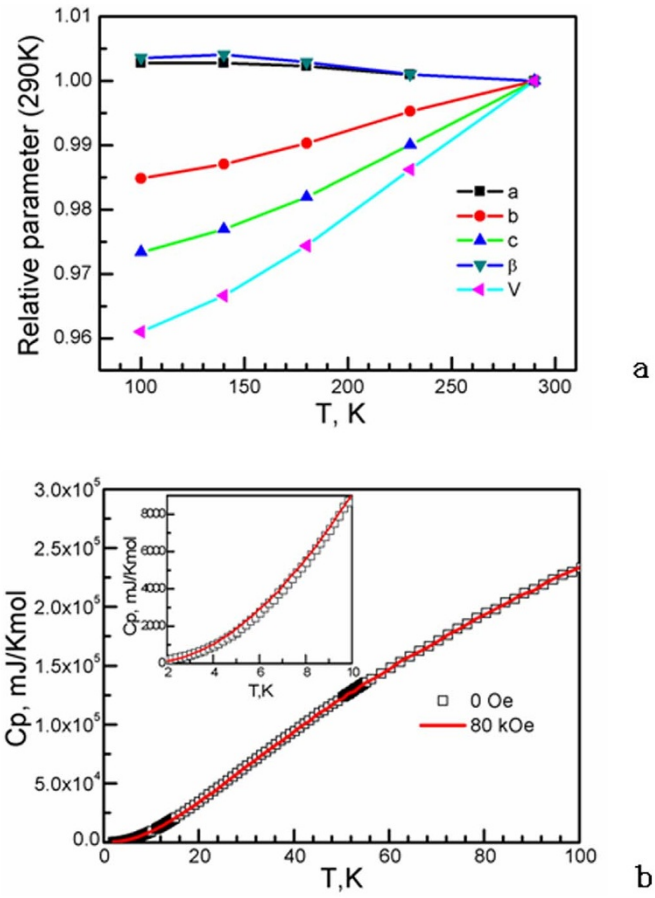

Figure 2 | (a) Temperature-dependent cell parameters from 290 K to 100 K. (b) Specific heat data of **1** under 0 Oe (empty black square) and 80 kOe(red solid line). Inset, low-temperature range.

angles are in the range 78.88 ~ 100.44(9)° for Cu1 and 77.99(9) ~ 98.29(9)° for Cu2, and the trans O–Cu–O angles are in the range 162.86(9) ~ 175.94(1)° for Cu1 and 162.27(8) ~ 174.88(10)° for Cu2. The oxalate-bridged Cu1···Cu2 distances are 5.5179(7) Å, 5.3593(6) Å and 5.3317(6) Å. The distance between the metal atoms separated by two oxalate anions inside a hexagonal ring vary from Cu1···Cu1 8.8801(7) Å and 9.3696(5) Å, Cu2···Cu2 9.7736(6) Å and 9.3696(5) Å. When temperature decreased, the Cu···Cu distance expanded along the *a* axis and contracted along the *b* axis. There are two enantiomers coexisting in the crystal: the Λ enantiomer (Cu1) and Δ enantiomer (Cu2) in one layer, and the Δ enantiomer (Cu1) and Λ enantiomer (Cu2) in another layer which are separated by cation and H_2O. It is the same situation as found in the charge-transfer salts with honeycomb lattice $[Cu_2(C_2O_4)_3^{2-}]_n$[38]. It is different from the coordination network isomerism of $[Cu_2(C_2O_4)_3^{2-}]_n$ in the (10,3) lattice, the configurations of Cu1 and Cu2 remain same as there are only the Δ enantiomer Cu1 and the Λ enantiomer Cu2 in a hyperhoneycomb lattice[40].

Specific heat measurement. No λ-peak was observed from temperature dependent specific heat data from 200 K to 2 K under 0 Oe and 80 kOe (Figure 2b). So there is no evidence for a structural or magnetic transition from 200 K to 2 K. The crystal structure at 2 K is the same as the crystal structure at 290 K. The value of heat capacity at 2 K is 183 mJ K^{-1} mol^{-1}.

Magnetic properties. On the χ-*vs*-T plot with the temperature decreasing, a broad maximum was observed at 52 K, and a turning point was observed at 14 K, then the χ value increased quickly and reached 0.0084 cm^3mol^{-1} at 2 K. At 300 K, the χT value is 0.465 cm^3 K mol^{-1}, it is higher than 0.375 cm^3Kmol^{-1} of an isolated Cu^{2+} with S = 1/2, and in the range of Cu^{2+} compounds with S = 1/2[41]. The data above 80 K was fitted to the Curie-Weiss law with C = 0.650(2) cm^3 mol^{-1} and $\theta = -120$ (1) K. No bifurcation was observed from ZFC/FC/RM measurement above 2 K. This is consistent with the specific heat experiment showing no long-range magnetic ordering and indicates the absence of spin glass freezing[20]. The isothermal magnetization at 2 K increased in a smooth curve and reached 0.012 N_β at 10 kOe, then the magnetization increased linearly and reached 0.044 N_β at 65 kOe (Figure 3).

Discussion

The distance between two anion layers which are separated by cation and H_2O is longer than 3.5 Å, so there is no significant interaction between two-dimensional anion layers. The starting point for understanding the magnetic properties is therefore consideration of the independent two-dimensional honeycomb layers.

The magnetic configuration of the honeycomb lattice can be postulated from an orbital analysis[42–44]. The unpaired electron exists in the magnetic orbital dx^2-y^2 on the equatorial plane. The orbital along the elongated octahedral Cu(II) is the dz^2 orbital as highlighted by black solid lines in Figure 1e, and the dz^2 orbital is perpendicular to the equatorial plane and the dx^2-y^2 orbital. The relationship between magnetic and structural properties of oxalate-bridged Cu^{2+} atoms was well established from one-dimensional Cu-oxalate compounds, for example, a ferromagnetic interaction was observed in $[Cu(bpy)(C_2O_4)](H_2O)_2$ when dx^2-y^2 orbitals on two oxalate-bridged Cu^{2+} atoms are parallel each other. Meanwhile, an antiferromagnetic interaction appeared when dx^2-y^2 orbitals on two oxalate-bridged Cu^{2+} atoms are perpendicular to each other[45–46]. Ferromagnetic interaction along the *b* axis between oxalate-bridged Cu1 and Cu2 and antiferromagnetic interaction along the *a* axis between oxalate-bridged Cu1 and Cu2 were assumed. Because the antiferromagnetic interaction is stronger than the ferromagnetic interaction between oxalate-bridged Cu^{2+} atoms, antiferromagnetic behavior should be expected in **1** and the magnetic configuration of **1**, if it orders, would be that of a system with a stripy antiferromagnetic ground state with a pair of spins up and a pair of spins down alternately on the honeycomb lattice (Figure 1c). This is distinct from the other possible magnetic configurations of honeycomb lattices (Figure 1a,b,d) and the stripy configuration is suggested by theoretical calculations to be the best candidate to lead to a quantum spin liquid[47–49].

On the χ-*vs*-T plot, a broad maximum at 52 K indicates short-range antiferromagnetic interactions in the low-dimensional system of metal atoms. The data above 2 K was fitted to several models: first the anisotropic honeycomb model of Curély et al, which showed good consistency with the orbital analysis above, giving an FM inter-chain interaction that is around 700 times weaker than the AF intra-chain coupling[50]. The best fit to the data was however given by the 1D Bonner-Fisher model plus a small impurity term, indicating a highly 1D state. This strongly 1D state may be the result of weak interchain coupling plus a further frustration of the interchain coupling J' by the second nearest neighbour interactions J'' (Figure 4)[51]. The parameters obtained from the fitting are: C = 0.4383(8) cm^3mol^{-1}, J = -43.82(7) K, $n_{impurity}$ = 1.09(2)%, $\theta_{impurity}$ = 1.27(3) K. From the value of J and the absence of magnetic ordering above 2 K we can provide an upper bound on the J'/J ratio of 2.2×10^{-2}, around half that of the benchmark S = 1/2 Heisenberg antiferromagnetic chain system $KCuF_3$[24].

The specific heat data shows that neither magnetic ordering, nor a structural transition happened between 200 K and 2 K. The crystal structure at 2 K should be same as the crystal structure at 290 K, so the magnetic configuration remains in the stripy antiferromagnetic mode to 2 K. The value of the heat capacity at 2 K is 183 mJ K^{-1} mol^{-1}, which is higher than the value in long-range magnetic ordered

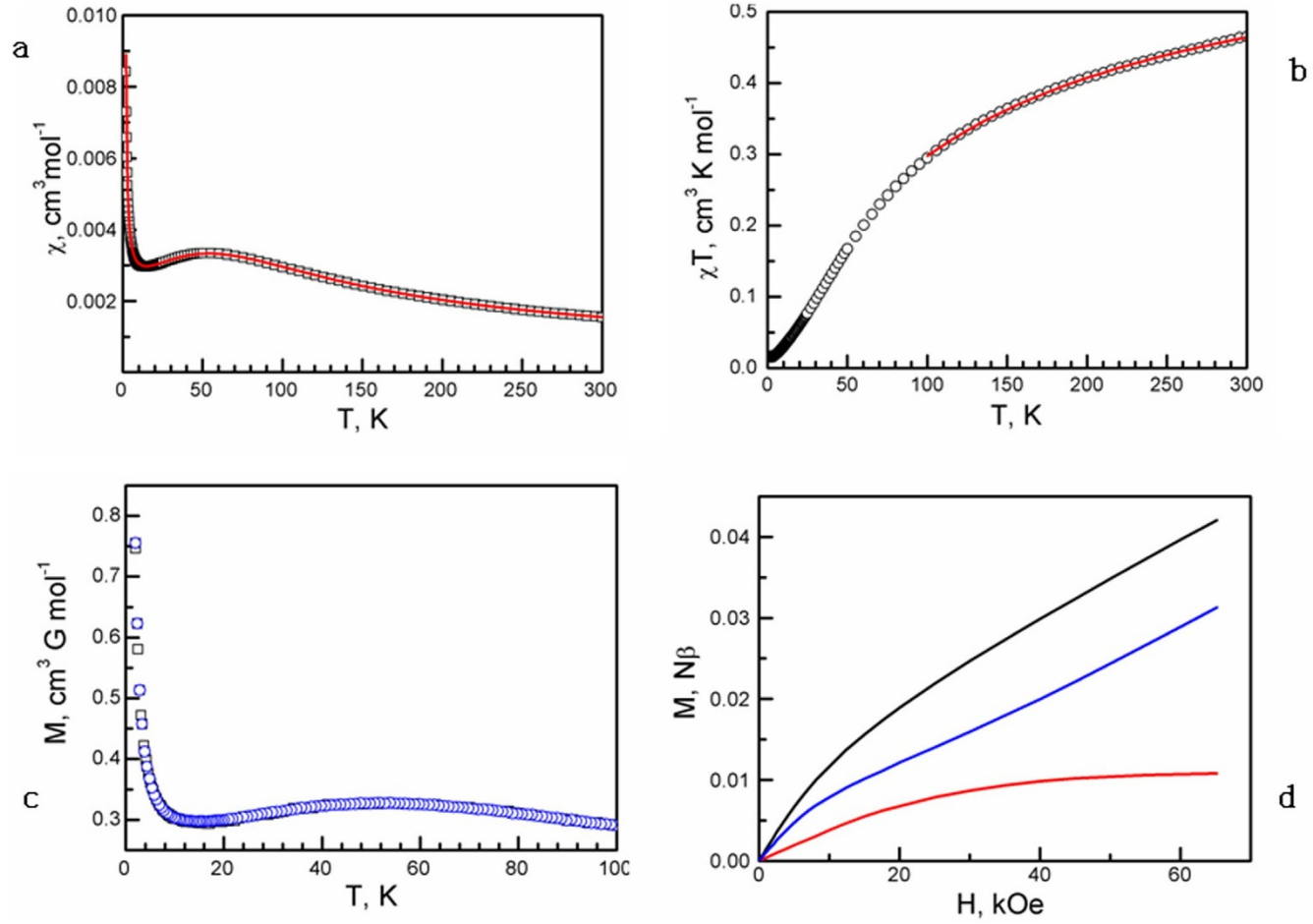

Figure 3 | Magnetic characterization of 1: (a) χ-vs-T (black empty square) of 1 under an applied field of 1000 Oe, the red line is a fit to the Bonner-Fisher law plus an impurity term. (b) χT-vs-T plot (black empty circle) of **1** under an applied field of 1000 Oe, the red line is a fit to the Curie-Weiss law. (c) ZFCM (black empty square) and FCM (blue empty circle) under 100 Oe. (d) Isothermal magnetization at 2 K. The black line is experimental data, the red line is the contribution from impurity, the blue line is experimental data after subtraction of the impurity contribution.

metal-oxalate-honeycomb compounds where the electron spins are frozen into an ordered array of magnetic dipoles. For example, it is 2.17 mJ K^{-1} mol^{-1} in Fe^{2+} ($S = 2$), and 43 mJ K^{-1} mol^{-1} in Co^{2+} ($S = 3/2$). Although there is a strong spin-orbital coupling in the Co^{2+} ($S = 3/2$) case, it is not a candidate spin liquid as it undergoes long range magnetic ordering at 21 K[52]. So the large heat capacity of **1** at 2 K suggests that the spins are in a quantum fluctuating spin liquid state[53].

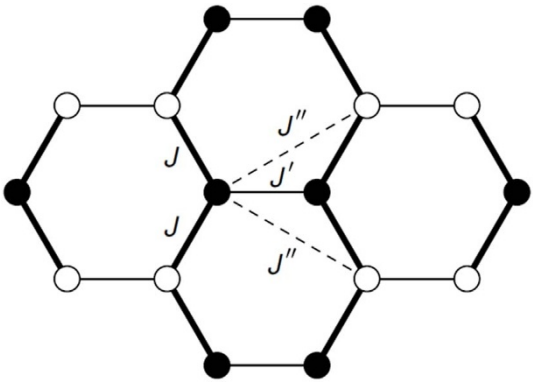

Figure 4 | **Magnetic interactions in 1.** Strong AF interactions J along the vertical chains and weak ferromagnetic interactions J' between the chains. An antiferromagnetic second nearest neighbour interchain coupling J'' leads to frustration of the already weak interchain coupling, leading to the highly 1D properties observed experimentally.

1 is different from reported low-dimensional octahedral coordinated Cu^{2+} compounds where the strong antiferromagnetic interaction and high f value were the result of interchain or interlayer interactions between Cu^{2+} atoms. For example in $CuCl_2$(1,4-dioxane)$(H_2O)_2$, the hydrogen bonds through O–H···Cl between chains results in strong antiferromagnetic interaction with θ = -71.9 K, but spin frustration has not been observed[54]. **1** is an antiferromagnetic compound that our measurements suggest to be candidate for the 1D class of quantum spin liquids. In this case the combination of dimensional reduction and frustration turns a honeycomb system into one where the properties of well-isolated chains dominate the magnetic properties[55–57].

Methods

Sample preparation and X-ray diffraction experiments. Blue thin crystal plates of $[(C_3H_7)_3NH]_2[Cu_2(C_2O_4)_3](H_2O)_{2.2}$ (**1**) were obtained from methanol solution of $Cu(NO_3)_2{\cdot}3H_2O$, $H_2C_2O_4{\cdot}2H_2O$ and $(C_3H_7)_3N$ in a 1 : 3 : 5 ratio at room-temperature with yield of 31%. Element analysis: $C_{24}H_{48.4}O_{14.2}N_2Cu_2$, F.W. = 719.345, calc. C 40.07, H 6.78, N 3.89; exp. C 40.45, H 6.82, N 3.91. A piece of single crystal was selected for single-crystal X-ray diffraction experiments at 290 K, 230 K, 180 K, 140 K and 100 K.

Specific heat measurement. The specific heat experiments were carried out on a Quantum Design PPMS-9XL system from 200 K to 2 K under 0 Oe and 80 kOe. The polycrystal was fixed on the sample stage with N-grease. The contribution from sample stage and N-grease was subtracted from the raw data.

Magnetic measurement. The magnetization measurement was performed using a tightly packed 16.26 mg polycrystalline sample which was sealed by 5.62 mg parafilm in capsule on a Quantum Design MPMS-7XL SQUID system. Susceptibility data were corrected for diamagnetism of sample by Pascal constants (-190.4×10^{-6} $cm^3\,mol^{-1}$ per Cu^{2+}) and the background was determined by a measurement of the sample holder.

1. Anderson, P. W. Resonating Valence Bonds: A New Kind of Insulator. *Mater. Res. Bull.* **8**, 153–160 (1973).
2. Balents, L. Spin liquids in frustrated magnets. *Nature* **464**, 199–208 (2010).
3. Ramirez, A. P. Strongly Geometrically Frustrated Magnet. *Annu. Rev. Mater. Sci.* **24**, 453–480 (1994).
4. Aeppli, G. & Chandra, P. Seeking a Simple Complex System. *Science* **275**, 177–178 (1997).
5. Lee, P. A. An End to the Drought of Quantum of Spin Liquids. *Science* **321**, 1306–1307 (2008).
6. Anderson, P. W. Resonating Valence Bond State in La_2CuO_4 and superconductivity. *Science* **235**, 1196–1198 (1987).
7. Jin, K., Butch, N. P., Kirshenbaum, K., Paglione, J. & Greene, R. L. Link between spin fluctuations and electron pairing in copper oxide superconductors. *Nature* **476**, 73–75 (2011).
8. Schlickum, U. *et al.* Chiral Kagome Lattice from Simple Ditopic Molecular Bricks. *J. Am. Chem. Soc.* **130**, 11778–11782 (2008).
9. Moulton, B., Lu, J., Hajndl, R., Hariharan, S. & Zaworotko, M. Crystal Engineering of Nanoscale Kagome Lattice. *Angew. Chem. Int. Ed.* **41**, 2821–2824 (2002).
10. Li, G. *et al.* $La_4Cu_{3-x}Zn_xMoO_{12}$: Zinc-Doped Cuprates with Kagome Lattices. *J. Am. Chem. Soc.* **127**, 14094–14099 (2005).
11. Wang, X., Wang, L., Wang, Z. & Gao, S. Solvent-Tuned Azido-Bridged Co^{2+} Layers: Square, Honeycomb, and Kagome. *J. Am. Chem. Soc.* **128**, 674–675 (2006).
12. Behera, J. N. & Rao, C. N. R. A Ni^{2+} (S = 1) Kagome compound Templated by 1,8-Diazacubane. *J. Am. Chem. Soc.* **128**, 9334–9335 (2006).
13. Zheng, Y. *et al.* A "Star" Antiferromagnet: A Polymeric Iron(III) Acetate That Exhibits Both Spin Frustration and Long-Range Magnetic Ordering. *Angew. Chem. Int. Ed.* **46**, 6067–6080 (2007).
14. Nytko, E., Helton, J., Muller, P. & Nocera, D. A Structurally Perfect S = 1/2 Metal-Organic Hybrid Kagome Antiferromagnet. *J. Am. Chem. Soc.* **130**, 2922–2923 (2008).
15. Lhotel, E. *et al.* Domain-Wall Spin Dynamics in Kagome Antiferromagnets. *Phy. Rev. Lett.* **107**, 257205 (2011).
16. Pratt, F. L. *et al.* Magnetic and non-magnetic phases of quantum spin liquid. *Nature* **471**, 612–616 (2011).
17. Yamashita, M. *et al.* Highly Mobile Gapless Excitations in a Two-Dimensional Candidate Quantum Spin Liquid. *Science* **328**, 1246–1248 (2010).
18. Isono, T. *et al.* Gapless Quantum Spin Liquid in an Organic Spin-1/2 Triangular-Lattice k-H_3(Cat-EDT-TTF)$_2$. *Phy. Rev. Lett.* **112**, 177201 (2014).
19. Sheckelton, J. P., Neilson, J. R., Soltan, D. G. & McQueen, T. M. Possible valence-bond condensation the frustrated cluster magnet $LiZn_2Mn_3O_8$. *Nat. Mater.* **11**, 493–496 (2012).
20. Shores, M., Nytko, E., Bartlett, B. & Nocera, D. A Structurally Perfect S = 1/2 Kagome Antiferromagnet. *J. Am. Chem. Soc.* **127**, 13462–13463 (2005).
21. Lee, S. *et al.* Quantum-spin-liquid states in the two-dimensional Kagome antiferromagnets $Zn_xCu_{4-x}(OD)_6Cl_2$. *Nat. Mater.* **6**, 853–859 (2007).
22. Han, T. *et al.* Fractionalized excitations in the spin-liquid state of a Kagome-lattice antiferromagnet. *Nature* **492**, 406–410 (2012).
23. Aidoudi, F. *et al.* An ionothermally prepared S = 1/2 vanadium oxyfluoride Kagome lattice. *Nat. Chem.* **3**, 801–806 (2011).
24. Tennant, D. A., Cowley, R. A., Nagler, S. E. & Tsvelik, A. M. Measurement of the spin-excitation continuum in one-dimensional $KCuF_3$ using neutron scattering. *Phy. Rev. B.* **52**, 13368 (1995).
25. Stone, M. B. *et al.* Extended Quantum Critical Phase in a Magnetized Spin-1/2 Antiferromagnetic Chain. *Phy. Rev. Lett.* **91**, 037205 (2003).
26. Lee, P. A. An End to the Drought of Quantum of Spin Liquids. *Science* **321**, 1306–1307 (2008).
27. Mattsson, A., Frojdh, P. & Einarsson, T. Frustrated honeycomb Heisenberg antiferromagnet: A Schwinger-boson approach. *Phy. Rev. B* **49**, 3997–4002 (1994).
28. Kitaev, A. Anyons in an exactly solved model and beyond. *Ann. Phy.* **321**, 2–111 (2006).
29. Pachos, J. K. The wavefunction of an anyon. *Ann. Phy.* **322**, 1254–1264 (2007).
30. Schmidt, K. P., Dusuel, S. & Vidal, J. Emergent Fermions and Anyons in the Kitaev Model. *Phy. Rev. Lett.* **100**, 057208 (2008).
31. Dusuel, S., Schmidt, K. P. & Vidal, J. Creation and Manipulation of Anyons in the Kitaev Model. *Phy. Rev. Lett.* **100**, 177204 (2008).
32. Liu, X. *et al.* Long-range magnetic ordering in Na_2IrO_3. *Phy. Rev. B.* **83**, 220403 (2011).
33. Onishi, N. *et al.* Magnetic ground state of the frustrated honeycomb antiferromagnet $Bi_3Mn_4O_{12}(NO_3)$. *Phy. Rev. B.* **85**, 184412 (2012).
34. Viciu, L. *et al.* Structure and basic magnetic properties of the honeycomb lattice compounds $Na_2Co_2TeO_6$ and $Na_3Co_2SbO_6$. *J. Sol. Stat. Chem.* **180**, 1060–1067 (2007).
35. Yamashita, T., Ohara, S. & Sakamoto, I. Magnetic properties of two-dimensional honeycomb lattice magnet RNi_3Al_9(R = Ga to Ln). *J. Phy. Soc. Jpn.* **80**, SA080 (2011).
36. Roudebush, J. H. *et al.* Structure and Magnetic Properties of $Cu_3Ni_2SbO_6$ and $Cu_3Co_2SbO_6$ Delafossites with honeycomb lattices. *Inorg. Chem.* **52**, 6083–6085 (2013).
37. Igarashi, K. *et al.* Absence of Magnetic Order in Ising Honeycomb-Lattice $Ba_3Co_2O_6(CO_3)_{0.7}$. *J. Phy. Con. Ser.* **400**, 032024 (2012).
38. Zhang, B., Zhang, Y. & Zhu, D. (BEDT-TTF)$_3$Cu$_2$(C$_2$O$_4$)$_3$(CH$_3$OH)$_2$: an organic-inorganic hybrid antiferromagnetic semiconductor. *Chem. Commun.* **48**, 197–199 (2012).
39. Shang, R., Xu, G., Wang, Z. & Gao, S. Phase Transitions, Prominent Dielectric Anomalies, and Negative Thermal Expansion in Three High Thermally Stable Ammonium Magnesium–Formate Frameworks. *Chem. Eur. J.* **20**, 1146–1158 (2014).
40. Zhang, B., Zhang, Y. & Zhu. D. $[(C_2H_5)_3NH]_2Cu_2(C_2O_4)_3$: a three-dimensional metal–oxalato framework showing structurally related dielectric and magnetic transitions at around 165 K. *Dalton Trans.* **14**, 8509–8511 (2012).
41. Carlin, R. L. & Van Duyneveld, A. L. *Magnetic Properties of Transition Metal Compounds.* Springer, New York (1977).
42. Kanamori, J. Crystal Distortion in Magnetic Compounds. *J. Appl. Phys.* **31**, 14S–23S (1960).
43. Kashida, S. Successive Jahn-Teller Phase Transitions in $K_2Pb_2Cu(NO_2)_6$. *J. Phys. Soc. Jpn.* **45**, 414–421 (1978).
44. Kahn, O. & Charlot, M. F. Overlap Density in Binuclear Complexes: A Topological Approach of the Exchange Interaction. *Nouv. J. Chim.* **4**, 567–576 (1980).
45. Oshio, H. & Nagashima, U. Design of a Homonuclear Ferromagnetic Chain: Structures and Magnetic Properties of Oxalato-Bridged Copper (II) Complexes with One-Dimensional Structures. *Inorg. Chem.* **31**, 3295–3301 (1992).
46. Castillo, O., Luque, A., Roman, P., Lloret, F. & Julve, M. Syntheses, Crystal Structures, and Magnetic Properties of One-Dimensional Oxalato-Bridged Co(II), Ni(II) and Cu(II) Complexes with n-Aminopyridine (n = 2–4) as Terminal Ligand. *Inorg. Chem.* **40**, 5526–5535 (2001).
47. Chaloupka, J., Jackeli, G. & Khaliullin, G. Kitaev-Heisenberg Model on a Honeycomb Lattice: Possible Exotic Phases in Iridium Oxides A_2IrO_3. *Phy. Rev. Lett.* **105**, 027204 (2010).
48. Reuther, J., Thomale, R. & Trebst, S. Finite-temperature phase diagram of the Heisenberg-Kitaev model. *Phy. Rev. B* **84**, 100406 (2011).
49. Price, C. C. & Perkins, N. B. Critical Properties of the Kitaev-Heisenberg Model. *Phy. Rev. Lett.* **109**, 187201 (2012).
50. Curely, J., Lloret, F. & Julve, M. Thermodynamics of the two-dimensional Heisenberg classical honeycomb lattice. *Phy. Rev. B.* **58**, 11465 (1998).
51. Bonner, J. C. & Fisher, M. E. Linear Magnetic Chains with Anisotropic Coupling. *Phy. Rev.* **135**, A640–A658 (1964).
52. Duan, Z., Zhang, Y., Zhang, B. & Zhu, D. Two Homometallic Ferrimagnets based on Oxalato-Bridged Honeycomb Assemblies: $(A)_2M^{II}_2(C_2O_4)_3$ (A = Ammonium Salt Derived from Diethylenetriamine; M^{II} = Fe^{2+}, Co^{2+}). *Inorg. Chem.* **48**, 2140–2146 (2009).
53. Yamashita, S. *et al.* Thermodynamic properties of a spin-1/2 spin-liquid state in a κ-type organic salt. *Nat. Phys.* **4**, 459–462 (2008).
54. Zhang, B., Zhu, D., Zhang, Y. Crystal-to-Crystal Transformation from a Mononuclear Compound in a Hydrogen-Bonded Three-Dimensional Framework to a Layered Coordination Polymer. *Chem. Eur. J.* **16**, 9994–9997 (2010).
55. Meng, Z. Y., Lang, T. C., Wessel, S., Assaad, F. F. & Mutamatsum, A. Quantum spin liquid emerging in two-dimensional correlated Dirac ferimions. *Nature* **464**, 847–851 (2010).
56. Gu, Z. *et al.* Time-reversal symmetry breaking superconducting ground state in the doped Mott insulator on the honeycomb lattice. *Phy. Rev. B.* **88**, 155112 (2013).
57. Clark, B. K., Abanin, D. A. & Sondhi, S. L. Nature of Spin Liquid State of the Hubbard Model on a Honeycomb Lattice. *Phy. Rev. Lett.* **107**, 087204 (2011).

Acknowledgments

We thank Prof. Lu Li, Liang Yin, Neil Sullivan for valuable discussion. This work was finical supported by NSFC. 21173230, the National Program on Key Basic Research Project: 2011CB932302 and 2013CB933402, the Strategic Priority Research Program of the Chinese Academy of Sciences: XDB12030100, P. R. China.

Author contributions

B.Z. and D.Z. managed the project. Magnetic measurement was carried out by Y.Z., single crystal X-ray diffraction experiment was carried out by Z.W., heat capacity measurement was carried out by D.W. B.Z. synthesised crystal, conducted all experiments and analyzed the data. Paper was written with discussion of B.Z., P.J.B., F.L.P. and D.Z.. B.Z., P.J.B. and F.L.P. wrote the main manuscript text. B.Z. prepared figures 1–3 and F.L.P. prepared figure 4. All authors reviewed the manuscript.

Additional information

Supplementary information accompanies this paper at http://www.nature.com/scientificreports

Competing financial interests: The authors declare no competing financial interests.

How to cite this article: Zhang, B. *et al*. Candidate Quantum Spin Liquid due to Dimensional Reduction of a Two-Dimensional Honeycomb Lattice. *Sci. Rep.* **4**, 6451; DOI:10.1038/srep06451 (2014).